CHAPTER 374

NUMERICAL PREDICTION OF BREAKING WAVES AND CURRENTS WITH A BOUSSINESQ MODEL

Okey George Nwogu[1]

ABSTRACT

This paper describes the extension of a comprehensive numerical model for simulating the propagation and transformation of ocean waves in coastal regions and harbours to include wave breaking, runup and breaking-induced currents. The numerical model is based on a time-domain solution of a fully nonlinear set of Boussinesq-type equations for wave propagation in intermediate and shallow water depths. The equations are able to describe most of the phenomena of interest in the nearshore zone including shoaling, refraction, diffraction, reflection, wave directionality and nonlinear wave-wave interactions. The Boussinesq model is extended to the surf and swash zones by coupling the mass and momentum equations with a one-equation model for the temporal and spatial evolution of the turbulent kinetic energy produced by wave breaking. The waves are assumed to start breaking when the horizontal component of the orbital velocity at the wave crest exceeds the phase velocity of the waves. Numerical and experimental results are presented for the shoaling and runup of regular and irregular waves on a constant slope beach and wave-induced currents behind a detached breakwater.

1. INTRODUCTION

The processes of wave breaking, runup, setdown and setup of the mean water level, turbulent energy production, generation of nearshore currents and generation of infragravity waves are important driving mechanisms for the transport of sediments and pollutants in coastal regions. A full mathematical description of the complex hydrodynamics in the surf and swash zones is difficult due to the highly nonlinear and turbulent nature of flow. By making different simplifying assumptions, however, numerous mathematical models been developed which reproduce with varying degrees of success the different hydrodynamic phenomena that occur in the surf and swash zones.

For waves propagating over simple bathymetries where shoaling, refraction and breaking are the dominant wave transformation processes, models based on the conservation of energy flux with an appropriate energy dissipation term have successfully been used to model the wave height variation in the surf zone (e.g. Battjes and Janssen 1978, Dally et al. 1985). Battjes and Janssen (1978) used a hydraulic jump analogy to derive

[1]Canadian Hydraulics Centre, National Research Council, Ottawa, Canada K1A 0R6

the form of dissipation term while Dally et al. (1985) assumed that the dissipation rate was proportional to the difference between the local energy flux and a stable energy flux. Similar energy dissipation terms have also been incorporated into the mild-slope equation (e.g. Isobe 1987, Özkan and Kirby 1993).

Most surf zone wave transformation models are based on time-averaged integral wave properties and do not follow the breaking process in a time dependent manner. For applications such as irregular wave propagation and sediment transport over barred beaches, time domain modeling provides a more accurate description of the breaking and reformation process. A time-dependent breaking model is also able to simulate the transition region after the onset of wave breaking, where there is a rapid decay in wave energy with almost no change in the setdown of the mean water level. The transition zone plays an important role in the prediction of wave-induced currents and sediment transport in the surf zone (Nairn et al., 1990).

Time-dependent numerical models based Boussinesq-type equations have successfully been used to simulate the nonlinear transformation of multidirectional ocean waves in intermediate and shallow water depths (e.g. Nwogu, 1994). Boussinesq equations can accurately describe most wave transformation processes outside the surf zone including shoaling, refraction, diffraction, reflection and nonlinear wave-wave interactions. Recently, several authors have extended Boussinesq models to simulate wave breaking in the surf zone including Zelt (1991), Karambas and Koutitas (1992), Schäffer et al. (1993), and Sato and Kabiling (1994). The models essentially incorporate a dissipative term due to turbulence stresses or the presence of a surface roller into the momentum equation. The models differ on how they treat the onset of breaking and the rate of wave energy dissipation.

In this paper, we employ a one-equation turbulence model to describe the temporal and spatial evolution of the turbulent kinetic energy produced by wave breaking. The waves are assumed to start breaking when the horizontal component of the orbital velocity at the wave crest exceeds the phase velocity of the waves. The rate of production of turbulent kinetic energy is assumed to be proportional to the vertical gradient of the horizontal water particle velocity at the wave crest. The time-dependent model is applicable to both periodic and non-periodic unidirectional and multidirectional waves.

One advantage of extending Boussinesq-type models to the surf zone is the ability to implicitly model interactions between hydrodynamic processes occurring at different time scales. Wave-induced currents and mean water level fluctuations are implicitly included in the wave propagation model and are derived from a time-average of the predicted velocities and surface elevation respectively, without having to explicitly calculate radiation stresses and separately solve a time-averaged hydrodynamic model.

2. THEORETICAL MODEL

2.1 Fully Nonlinear Boussinesq Equations

Boussinesq equations represent the depth-integrated equations for the conservation of mass and momentum for nonlinear dispersive waves, propagating in water of variable depth. The velocity potential, ϕ, can be expanded as power series in the vertical coordinate, z. An approximation is introduced for frequency dispersion by truncating the series at second-order, resulting in a quadratic variation for the horizontal velocity over depth, and a linear variation for the vertical velocity:

$$\begin{aligned} \mathbf{u}(z) &= \mathbf{u}_\alpha + (z_\alpha - z)\left[\nabla(\mathbf{u}_\alpha \cdot \nabla h) + (\nabla \cdot \mathbf{u}_\alpha)\nabla h\right] \\ &+ \left[\frac{(z_\alpha + h)^2}{2} - \frac{(z+h)^2}{2}\right]\nabla(\nabla \cdot \mathbf{u}_\alpha) \qquad (1) \\ w(z) &= -\left[\mathbf{u}_\alpha \cdot \nabla h + (z+h)\nabla \cdot \mathbf{u}_\alpha\right] \qquad (2) \end{aligned}$$

where $\nabla = (\partial/\partial x, \partial/\partial y)$, $h(\mathbf{x})$ is the water depth and $\mathbf{u}_\alpha = \nabla\phi|_{z=z_\alpha}$. Given a vertical profile for the flow field (Eqns. 1 & 2), the governing equations of fluid motion can be integrated over depth, reducing the three-dimensional problem to a two-dimensional one. The depth-integrated mass conservation equation can be written as:

$$\eta_t + \nabla \cdot \int_{-h}^{\eta} \mathbf{u}\, dz = 0, \qquad (3)$$

where $\eta(\mathbf{x}, t)$ is the free surface elevation. Although Boussinesq equations were originally derived for weakly nonlinear waves, a fully nonlinear variant of the equations was recently derived by Wei et al. (1995). The momentum equation, fully nonlinear up to the order of truncation of the dispersive terms, is derived from the dynamic boundary condition at the free surface as:

$$\begin{aligned} &\mathbf{u}_{\alpha t} + g\nabla\eta + (z_\alpha - \eta)\left[\nabla(\mathbf{u}_{\alpha t} \cdot \nabla h) + (\nabla \cdot \mathbf{u}_{\alpha t})\nabla h\right] \\ &+ \left[\frac{(z_\alpha + h)^2}{2} - \frac{(h+\eta)^2}{2}\right]\nabla(\nabla \cdot \mathbf{u}_{\alpha t}) + \frac{1}{2}\nabla(\mathbf{u}_s \cdot \mathbf{u}_s + w_s^2) \\ &-\left[(\mathbf{u}_{\alpha t} \cdot \nabla h) + (h+\eta)(\nabla \cdot \mathbf{u}_{\alpha t})\right]\nabla\eta + \frac{f_w}{(h+\eta)}\mathbf{u}_b|\mathbf{u}_b| + \frac{\partial}{\partial z}\left(\overline{\mathbf{u}'w'}\right) = 0 \qquad (4) \end{aligned}$$

where g is the gravitational acceleration, $\mathbf{u}_b = \mathbf{u}(-h)$, $\mathbf{u}_s = \mathbf{u}(\eta)$ and $w_s = w(\eta)$. Two additional terms have been introduced into the momentum equation to simulate the dissipation of wave energy due to bottom friction and wave breaking. f_w is an empirical bottom friction factor while $\overline{\mathbf{u}'w'}$ represents the shear stress due to breaking-induced turbulent velocity fluctuations (u', v', w'). A semi-empirical turbulence closure model (Section 2.2) is used to relate the turbulence stresses to the wave orbital velocities.

The elevation of the velocity variable z_α is a free parameter and is chosen to minimize the differences between the linear dispersion characteristics of the Boussinesq model and linear theory. An optimum depth for the velocity variable, $z_\alpha = -0.53h$, gives errors of less than 2% in the phase speed from shallow water depths up to the deep water depth limit.

2.2 Turbulence Model

Several turbulence models have been proposed for fluid flow problems (see review by Rodi, 1980). In this paper, the standard one-equation turbulence model is used to describe the spatial and temporal evolution of the turbulent kinetic energy, k, produced by wave breaking. We do not attempt to model details of the turbulent motion, but rather, investigate the effect of turbulence on the wave field.

The key assumptions made in developing the model are:

1. the breaking process is assumed to be "spilling"
2. turbulence is initiated in the wave crest region due to large vertical gradients of the horizontal velocity, $\partial \mathbf{u}/\partial z$
3. turbulence is produced only when the horizontal velocity at the wave crest exceeds the phase velocity of the waves
4. the rate of production of turbulent kinetic energy is proportional to the vertical gradient of the horizontal velocity at the wave crest
5. turbulence is primarily convected in the crest front region with the horizontal component of the orbital velocity at the crest

The Boussinesq eddy viscosity concept can be used to relate the turbulence shear stresses to the velocity gradients:

$$\overline{\mathbf{u}'w'} = -\nu_t \frac{\partial \mathbf{u}}{\partial z} \tag{5}$$

where ν_t is the eddy viscosity. By substituting the expression for $\mathbf{u}(z)$ given in equation (1), the dissipative term in the momentum equation (Eqn. 4) becomes:

$$\frac{\partial}{\partial z}\left(\overline{\mathbf{u}'w'}\right) = -\frac{\partial}{\partial z}\left(\nu_t \frac{\partial \mathbf{u}}{\partial z}\right) = \nu_t \nabla(\nabla \cdot \mathbf{u}_\alpha) \tag{6}$$

The rate of wave energy dissipation is thus governed by the magnitude of the eddy viscosity which is related to the turbulent kinetic energy, k, and a turbulence length scale, ℓ_t, by:

$$\nu_t = \sqrt{k}\,\ell_t \tag{7}$$

The turbulent kinetic energy is determined from a semi-empirical transport equation with a source term for turbulent kinetic energy production by wave breaking:

$$k_t + \mathbf{u}_s \cdot \nabla k = \nu_k \nabla^2 k + B\nu_t \left[\left(\frac{\partial u}{\partial z} \right)^2 + \left(\frac{\partial v}{\partial z} \right)^2 \right]_{z=\eta} - C_D \frac{k^{3/2}}{\ell_t} \tag{8}$$

The first term on the right hand side represents the horizontal diffusion of turbulent kinetic energy. This term is usually much smaller than the convective term, $\mathbf{u}_s \cdot \nabla k$. The second term represents the production of turbulent kinetic energy due to wave breaking. The parameter B is introduced to ensure that turbulence is produced only when horizontal velocity at the wave crest, u_s, exceeds the phase velocity of the waves, C, i.e.

$$B = \begin{cases} 0 & |\mathrm{u}_s| < C \\ 1 & |\mathrm{u}_s| \geq C \end{cases} \tag{9}$$

This criterion is valid for progressive waves and has been found to accurately predict the breaker location observed in experiments with regular waves shoaling on a constant slope beach. For irregular waves, an approximate phase velocity can be calculated using the average zero-crossing period, although an instantaneous phase velocity can also be determined using $C = -\eta_t / |\nabla \eta|$.

The last term on the right hand side of the transport equation (8) represents the dissipation of turbulent kinetic energy into heat. C_D is an empirical constant with a representative value of 0.08 for most turbulent shear flows (Rodi, 1980).

The rate of production of turbulent kinetic energy depends on ν_t which initially is unknown. Using the mixing length hypothesis which assumes a local balance between production and dissipation of turbulent kinetic energy, the value of ν_t for the production term is determined as:

$$\nu_t = \frac{\ell_t^2}{\sqrt{C_D}} \left[\left(\frac{\partial u}{\partial z} \right)^2 + \left(\frac{\partial v}{\partial z} \right)^2 \right]_{z=\eta}^{1/2} \tag{10}$$

By choosing an arbitrary value for C_D, the turbulence length scale ℓ_t becomes the only free parameter in the turbulence model which governs the rate of wave energy dissipation and turbulent kinetic energy production. ℓ_t is expected to be of the order of the wave height and is determined from comparisons of the numerical model results with experimental results.

2.3 Numerical Solution

The governing Boussinesq equations have been solved with an iterative Crank-Nicolson finite difference method, with a predictor-corrector scheme used to provide the initial estimate. The computational domain is discretized using a rectangular grid, with the dependent variables η, u_α and v_α defined at the grid points in a staggered manner. The numerical solution procedure consists of solving an algebraic expression for η at all grid points, tridiagonal matrices for u_α along lines in the x direction and tridiagonal matrices for v_α along lines in the y direction at every time step. An explicit second-order scheme is used for the turbulence transport equation. Details of the numerical solution technique can be found in Nwogu (1996).

The boundaries of the computational domain may be specified as wave input boundaries or solid walls. Along external or internal wave generation boundaries, time histories of $(u_\alpha, u_{\alpha,xx}, v_{\alpha,xy})$ or $(v_\alpha, v_{\alpha,yy}, u_{\alpha,xy})$, corresponding to periodic or non-periodic unidirectional or multidirectional sea states are input. Waves propagating out of the domain are artificially absorbed in damping regions placed next to solid wall boundaries. Artificial damping of wave energy is accomplished by introducing terms out of phase with the surface velocity and fluid acceleration into the continuity and momentum equations respectively.

A simple extrapolation scheme is used to simulate wave runup. Consider the one-dimensional case where the shoreline boundary condition is given by zero mass flux, or equivalently, $\eta_x = 0$. When the water surface elevation η_i at grid point i exceeds the elevation of an adjacent land point, h_{i+1}, we assume that the land point will be flooded at the next time step. The initial value of the water level on the the land point for the next time step is then extrapolated from the surface elevation at adjacent water points:

$$\eta_{i+1} = 4\eta_i - 3\eta_{i-1} \qquad \text{if } \eta_i > -h_{i+1} \tag{11}$$

Outputs of the numerical model are time histories of the surface elevation and two components of the horizontal velocity at desired grid points in the computational domain, corresponding frequency and directional wave spectra at those locations, the instantaneous water surface elevation at specified time steps, and the significant wave height distribution and time-averaged horizontal velocities over the entire computational domain.

3. NUMERICAL AND EXPERIMENTAL RESULTS

The numerical model was initially evaluated using data obtained from experiments carried out by Nwogu (1993) in the three-dimensional wave basin of the Canadian Hydraulics Center. A 1:25 constant slope concrete beach was constructed in the 30 m $\times$ 20 m $\times$ 3 m basin, equipped with a 60-segment directional wave generator. The toe of the slope was located 4.6 m away from the wave boards. The water depth in the constant depth portion of the basin was 0.56 m. Tests were carried out for a wide variety of regular and irregular, unidirectional and multidirectional waves. The water surface elevation along the centerline of the basin was measured with a linear array of 23 water level gauges. The experimental setup is described in greater detail by Nwogu (1993).

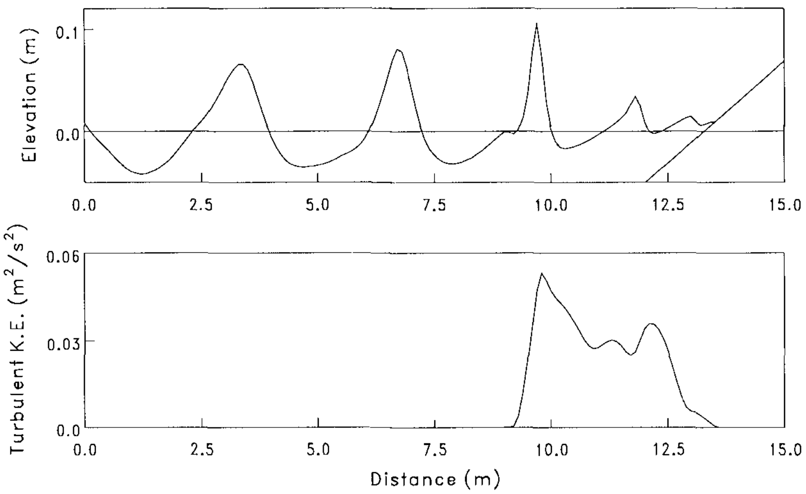

Figure 1. Breaking and runup of a regular wave ($T = 2$ s) on a 1:25 beach.

3.1 Shoaling of Regular Waves

The numerical model was used to investigate the shoaling and breaking of a regular wave with period, $T = 2$ s, and height, $H = 0.09$ m, on a 1:25 beach. The computations were carried out using a grid size $\Delta x = 0.1$ m and time step size $\Delta t = 0.04$ s. A bottom friction coefficient, $f_w = 0.01$, was used for all the computations. Figure 1 shows the spatial profile of the water surface elevation at an instant of time and the corresponding turbulent kinetic energy distribution. The turbulent kinetic energy is maximum close to the breaker location and decreases towards the shoreline. The turbulent kinetic energy exhibits an oscillatory behaviour in space due to the periodic nature of the production of turbulence from each breaking wave event.

Figure 2 shows a comparison of the measured and predicted time histories of the surface elevation at four water depths, both outside and inside the breaker zone. The numerical model is able to reproduce the highly asymetric wave profile in the surf zone. The spatial variation of the average zero-crossing wave height and mean water level are plotted in Figure 3. Fairly good agreement is obtained between the numerical and experimental results. A turbulence length scale $l_t = 0.35$ m with $C_D = 0.08$ gave the best match of rate of wave energy decay through the surf zone. The solution is not unique, however, as other combinations of C_D, ℓ_t, and the breaking criterion also give reasonable matches of the wave height decay. An extensive investigation is presently being carried out to recommend optimum values of the turbulence model parameters as a function of incident wave parameters.

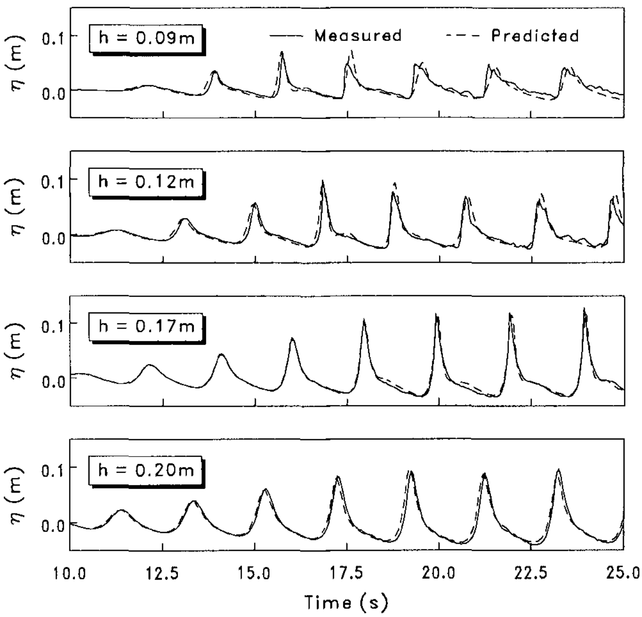

Figure 2. Measured and predicted time histories for a regular wave ($T = 2$ s) shoaling on a 1:25 beach.

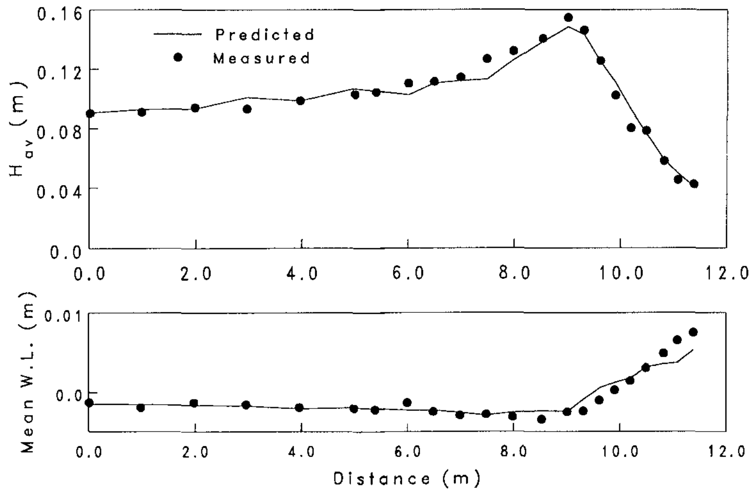

Figure 3. Measured and predicted spatial variation in wave height for a regular wave ($T = 2$ s) shoaling on a 1:25 beach.

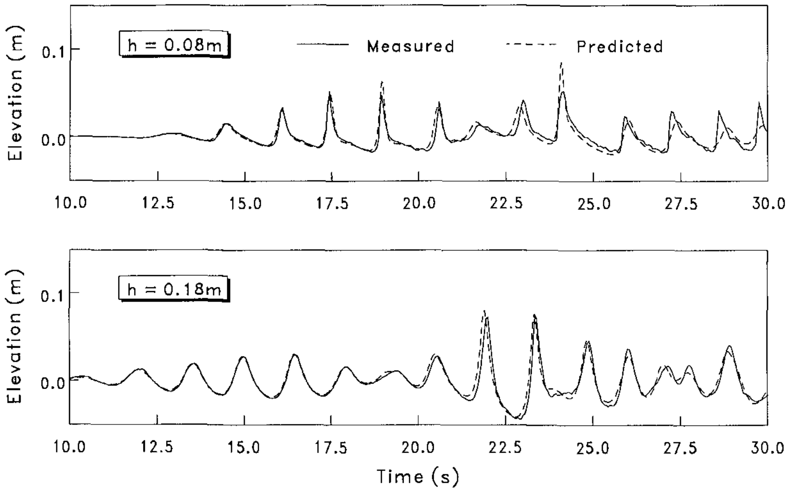

Figure 4. Measured and predicted water surface elevations for an irregular wave with T_p = 1.5 s shoaling on a 1:25 beach.

3.2 Shoaling of Irregular Waves

The numerical model was applied to the shoaling of an irregular wave train on the 1:25 beach. A sea state with a duration of 819.2 s was synthesized from a JONSWAP spectrum with significant wave height, H_{mo} = 0.09 m, peak period, T_p = 1.5 s, and peak enhancement factor, γ = 3.3, using the random phase method. The computations were carried out using Δx = 0.075 m, Δt = 0.025 s and ℓ_t = 0.1 m. Figure 4 shows a comparison of the measured and predicted water surface elevations at two shallow water depths. The numerical model is able to reproduce reasonably well the time-domain characteristics of individual wave breaking in an irregular wave train.

The spectral densities of the measured and predicted water surface elevation time histories at different water depths are compared in Figure 5. The spectral estimates were averaged over 0.04 Hz frequency bands. Fairly good agreement is obtained between the measured and predicted wave spectra. The numerical model is able to accurately describe the cross-spectral transfer of energy due to nonlinear wave-wave interactions as well as the decrease in wave energy through the surf zone.

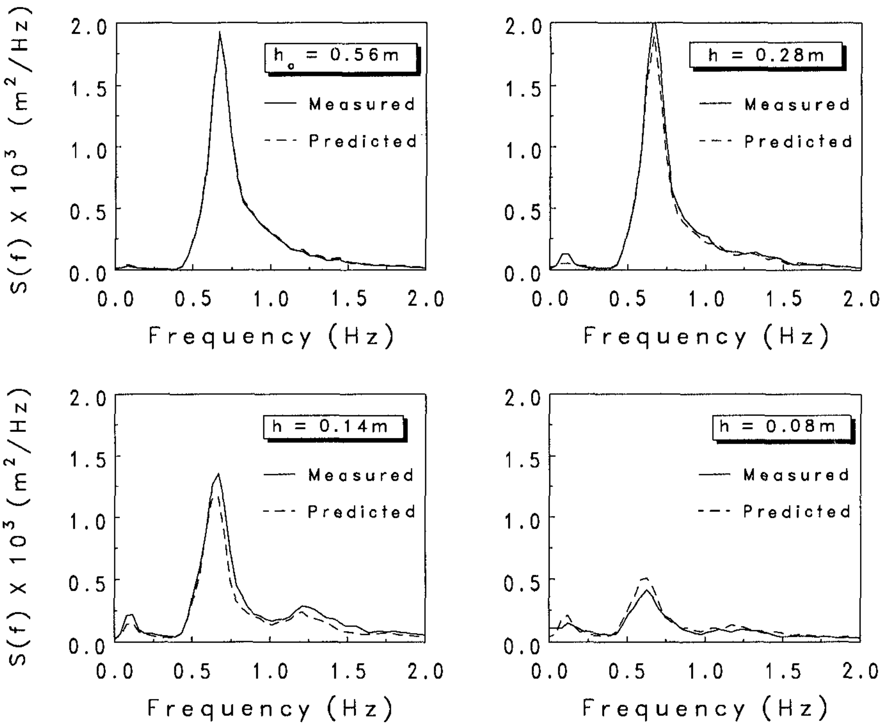

Figure 5. Spectral densities of surface elevation for an irregular wave with $T_p = 1.5$ s shoaling on a 1:25 beach.

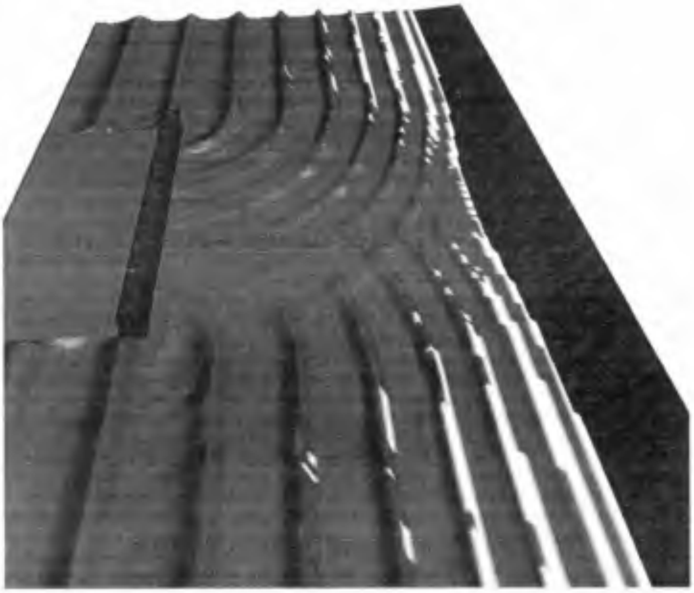

Figure 6. Three-dimensional view of the instantaneous water surface elevation around an offshore breakwater a 1:50 beach.

3.3 Wave-Induced Currents behind a Detached Breakwater

The calculation of currents induced by breaking waves is important in modeling the transport of sediments and pollutants in the surf zone. The two-dimensional Boussinesq model was used to investigate the generation of currents behind an offshore breakwater on a constant slope beach by shoaling and breaking waves. A generic example was used with a 400 m long breakwater placed 350 m from the shoreline on a 1:50 beach. A normally incident regular wave with period T = 10 s and height H = 2 m was generated at the 10 m depth. The computations were carried out with $\Delta x = \Delta y =$ 5 m, $\Delta t = 0.2$ s, and $f_w = 0.01$.

Figure 6 shows a three-dimensional view of the instantaneous water surface elevation around the offshore breakwater. Regions of the crest front with turbulent kinetic energy present have been highlighted in white. The predicted wave height distribution is shown in Figure 7 while the time and depth-averaged velocity pattern is shown in Figure 8. Two circulation cells are observed behind the detached breakwater. This pattern is qualitatively consistent with known observations of wave-induced currents and the formation of tombolos behind offshore breakwaters.

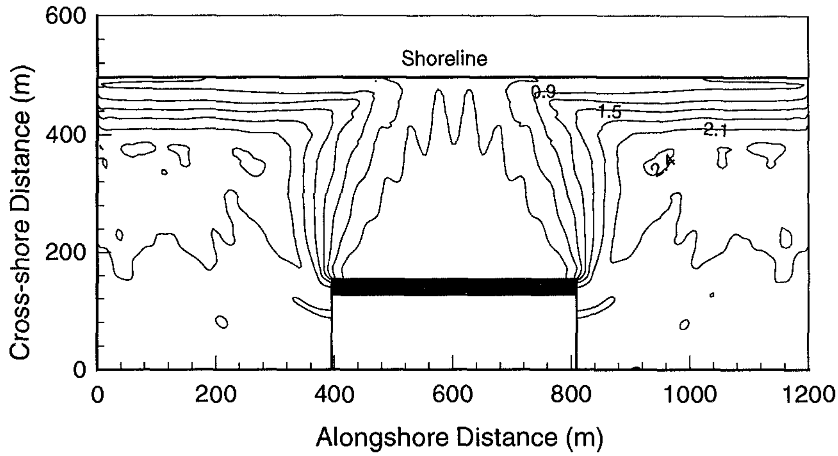

Figure 7. Average wave height distribution behind an offshore breakwater for a regular wave (T = 10 s, H = 2 m) shoaling on a 1:50 beach.

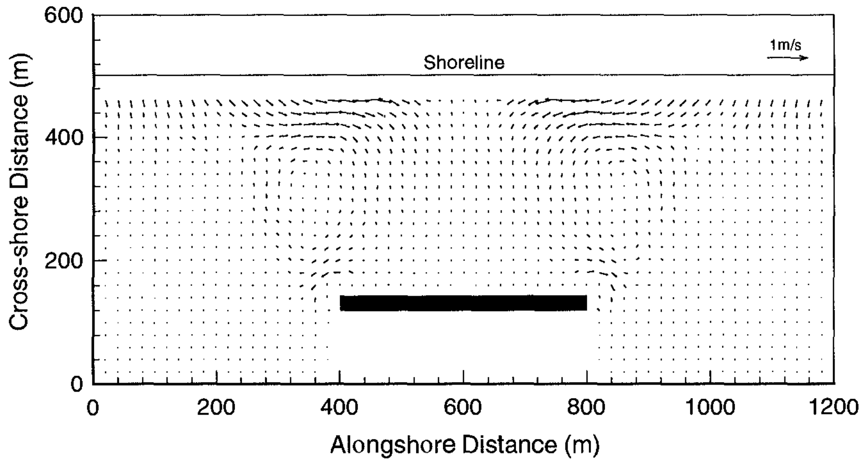

Figure 8. Predicted time and depth-averaged velocity behind an offshore breakwater for a regular wave (T = 10 s, H = 2 m) shoaling on a 1:50 beach.

4. CONCLUSIONS

A fully nonlinear Boussinesq wave propagation model has been extended to the surf and swash zones by coupling the mass and momentum equations with a one-equation turbulent kinetic energy transport model. The waves are assumed to start breaking when the horizontal velocity at the wave crest exceeds the phase velocity of the waves. The rate of production of turbulent kinetic energy is assumed to be proportional to the vertical gradient of the horizontal velocity at the wave crest. The numerical model has been compared to experimental data for the shoaling of regular and irregular waves on 1:25 beach. The model is able to reproduce reasonably well the frequency and time domain characteristics of waves in the surf zone. The results presented in this paper are of preliminary nature and further work is being carried to compare the numerical model with measured data on the spatial and temporal evolution of turbulence induced by wave breaking, the vertical distribution of currents in the surf zone, wave runup and nearshore circulation patterns.

REFERENCES

Battjes, J.A. and Janssen, J.P.F.M. 1978. Energy loss and setup due to breaking of random waves. *Proc. of the 16th Int. Conference on Coastal Engineering*, ASCE, Hamburg, 569-589.

Dally, W.R., Dean, R.G., and Dalrymple, R.A. 1985. Wave height variation across beaches of arbitrary profile. *Journal of Geophysical Research*, **90**(C6), 11917-11927.

Isobe, K. 1987. A parabolic equation model for transformation of irregular waves due to refraction, diffraction and breaking. *Coastal Engineering in Japan*, **30**, 33-47.

Karambas, Th. V. and Koutitas, C. 1992. A breaking wave propagation model based on Boussinesq equations. *Coastal Engineering*, **18**, 1-19.

Nairn, R.B., Roelvink, J.A., and Southgate, H.N. 1990. Transition zone width and implications for modelling surfzone hydrodynamics. *Proc. of the 22nd Int. Conference on Coastal Engineering*, ASCE, Delft, 68-81.

Nwogu, O. 1993. Alternative form of Boussinesq equations for nearshore wave propagation. *Journal of Waterway, Port, Coastal and Ocean Engineering*, ASCE, **119**(6), 618-638.

Nwogu, O. 1994. Nonlinear evolution of directional wave spectra in shallow water. *Proc. of the 24th Int. Conference on Coastal Engineering*, ASCE, Kobe, 467-481.

Nwogu, O. 1996. WaveSim™ - A comprehensive wave simulation model for coastal regions and harbours. *Canadian Hydraulics Centre Technical Report*, National Research Council, Canada (in preparation).

Rodi, W. 1980. Turbulence models and their application in hydraulics - A state of the art review. International Association for Hydraulic Research, Delft.

Sato, S., and Kabiling, M.B. 1994. A numerical simulation of beach evolution based on a nonlinear dispersive wave-current model. *Proc. of the 24th Int. Conference on Coastal Engineering*, ASCE, Kobe, 2557-2570.

Schäffer, H.A., Madsen, P.A., and Deigaard, R. 1993. A Boussinesq model for waves breaking in shallow water. *Coastal Engineering*, **20**, 185-202.

Özkan, H.T. and Kirby, J.T. 1993. Evolution of breaking directional spectral waves in the nearshore zone. *Proc. of the 2nd Int. Symposium on Ocean Wave Measurement and Analyis*, WAVES '93, ASCE, 849-863.

Wei, G., Kirby, J.T., Grilli, S.T., and Subramanya, R. 1995. A fully nonlinear Boussinesq model for surface waves. Part 1. Highly nonlincar unsteady waves. *Journal of Fluid Mechanics*, **294**, 71-92.

Zelt J.A. 1991. The run-up of nonbreaking and breaking solitary waves. *Coastal Engineering*, **15**, 205-246.